Rotationally resolved photoelectron spectroscopy of autoionizing states of water

W. L. Glab
Department of Physics, Texas Tech University, P. O. Box 41051, Lubbock, Texas 79409

M. S. Child
Department of Theoretical Chemistry, University of Oxford, 5 South Parks Road, Oxford OX1 3UB, United Kingdom

S. T. Pratt
Argonne National Laboratory, 9700 South Cass Avenue, Argonne, Illinois 60439

(Received 8 April 1998; accepted 22 May 1998)

Rotationally resolved photoelectron spectra are reported for rovibronically state-selected autoionizing levels of water. These photoelectron spectra are helpful for the spectroscopic assignment of the autoionizing levels and provide considerable dynamical information on the mechanisms for the transfer of energy and angular momentum between the ion core and the Rydberg electron. As a result of angular momentum restrictions, photoelectron spectra for $J=0$ autoionizing levels provide a direct partial wave analysis for the ejected photoelectrons. © *1998 American Institute of Physics.* [S0021-9606(98)00832-0]

I. INTRODUCTION

The spectroscopy and dynamics of the Rydberg states of water have attracted considerable recent attention as a result of progress in both experimental[1–4] and theoretical[5–10] methods. High resolution photoabsorption and photoionization spectra from the electronic ground state to Rydberg series converging to the $\tilde{X}\ ^2B_1$ and $\tilde{A}\ ^2A_1$ states of H_2O^+ have been recorded by using supersonic molecular beam sources[2] and vacuum ultraviolet (VUV) light generated by four-wave mixing in rare gases.[1,4] More recently, VUV-visible double resonance studies via the $\tilde{C}\ ^1B_1$ state have been performed to probe Rydberg series converging to excited vibrational levels of the H_2O^+ $\tilde{X}\ ^2B_1$ ground state.[11] From the theoretical perspective, the adaptation of multichannel quantum defect theory[12] to the Rydberg states of water[8] has resulted in a unified understanding of the 3d Rydberg states[9] and provided the theoretical underpinnings for the analysis of the high-resolution VUV spectra of Page *et al.*[1] and Vrakking *et al.*[4] Nevertheless, a complete analysis of these spectra and the double-resonance spectra of Glab[11] has not yet been achieved and efforts continue toward this end. VUV light generated by four-wave mixing has also been used to record rotationally resolved, zero-kinetic energy photoelectron spectra (ZEKE-PES) of water.[3,5–7] These spectra have been reproduced theoretically by McKoy and co-workers,[5–7] and provide considerable information on the rotational branching ratios and partial cross sections at threshold.

In this paper, rotationally resolved photoelectron spectra are reported for rotationally state-selected autoionizing levels of water, which were excited by two-color $(2+1')$ excitation via the $\tilde{C}\ ^1B_1$ (1,0,0) level. While such spectra have been reported previously[13,14] for H_2, and more recently[15,16] for NO, to our knowledge this is the first report of rotationally resolved photoelectron spectra of autoionizing levels of a polyatomic molecule. These spectra provide significant information on the dynamics of the autoionization process, which can be viewed as the inelastic scattering of the Rydberg electron off a state-selected (or nearly state-selected) ion core. In particular, rotationally resolved photoelectron spectra reveal significant details about the mechanisms for the conversion of rotational and vibrational energy of the ion core into electronic (and ultimately, translational) energy of the Rydberg (ejected) electron, as well as information on the partial wave composition of the outgoing photoelectron. The latter is particularly noteworthy for $J=0$ autoionizing levels because, in this case, each rotational level can be correlated with a specific value of ℓ of the photoelectron. The analysis of rotationally resolved photoelectron spectra can also provide important clues about the nature of the autoionizing level when its specific assignment is not known.

II. EXPERIMENT

The experiments were performed using a second generation magnetic bottle electron spectrometer that has been described previously.[17–19] In this instrument, ionization occurs in a diverging 1-T magnetic field that allows 50% collection efficiency of the photoelectrons while maintaining high resolution for time-of-flight analysis of the electron kinetic energy.[20] Resolution of 3.5 meV has been demonstrated with this instrument for 1-eV electrons produced by $(3+1')$ ionization of krypton. This resolution can vary somewhat depending on the alignment of the lasers, but the spectra reported here display comparable resolution. The present experiments were performed by using two homebuilt dye lasers pumped by the third-harmonic light from a single Nd^{+3}:YAG laser. The output of the first dye laser was frequency doubled in a β-barium borate crystal to generate approximately 50 μJ/pulse of light at approximately 239 nm

for the two-photon $\tilde{C}\ ^1B_1 \leftarrow\leftarrow \tilde{X}\ ^1A_1$ transition. This doubled light was separated from the fundamental by using dichroic mirrors and focused into the interaction region with a 75-mm focal-length lens. For the present experiments, which emphasize Rydberg states with $\tilde{X}\ ^2B_1$ (1,0,0) ion cores and principal quantum number $n=6$, the output of the second laser was tunable from 546 nm to 556 nm. Approximately 2 mJ/pulse of light from this laser was focused into the interaction region using a 25-cm focal-length lens, counterpropagating with the light from the pump laser. Both laser beams were polarized parallel to the magnetic field of the electron spectrometer and their optical pathlengths were arranged so that the two pulses were temporally overlapped in the interaction region. The wavelengths of the two lasers were calibrated by using the optogalvanic effect in a neon hollow-cathode lamp.

Water vapor from an effusive source flowed through the continuously pumped interaction region, providing a sample pressure of a few times 10^{-5} Torr. The photoelectron time-of-flight data for individual laser shots were recorded by sending the signal from a dual channelplate detector to a digital oscilloscope. The very low initial photoelectron energies made it necessary to apply a potential of ~ -0.5 V to a grid in the interaction region, in order to push the electrons into the flight tube of the spectrometer. The photoelectron spectra presented here represent the summed data for 5000–10 000 laser shots, and the time-of-flight spectra were converted to an energy scale as described previously. The photoelectron spectra for the autoionizing levels were calibrated by using the known energies of the photoelectrons produced by single-color (2+1) ionization to the H_2O^+ $\tilde{X}\ ^2B_1$ (0,0,0) and (1,0,0) levels and by assuming that the earliest photoelectron peak corresponded to the H_2O^+ $\tilde{X}\ ^2B_1$ (0,0,0) 0_{00} level.[21] This calibration, which is accurate to $\sim$2 to 3 meV, was confirmed by comparison with the known spacings among the lowest rotational energy levels of the H_2O^+ $\tilde{X}\ ^2B_1$ (0,0,0) state,[22] this being the only energetically accessible ionic vibrational level for the autoionizing states studied here.

The experiments were performed in three stages. First, the wavelength of the pump laser was scanned while the total one-color photoelectron signal was monitored, thus mapping out the structure of the two-photon $\tilde{C}\ ^1B_1$ (1,0,0) $\leftarrow \tilde{X}\ ^1A_1$ transition. The $\tilde{C}\ ^1B_1$ (1,0,0) state has been characterized previously by Ashford *et al.* by using (3+1) ionization spectroscopy,[23] and the resulting spectroscopic constants were used to assign the present two-photon $\tilde{C}\ ^1B_1$ (1,0,0) $\leftarrow \tilde{X}\ ^1A_1$ (0,0,0) pump transition. Although the $\tilde{C}\ ^1B_1$ (1,0,0) level is fairly strongly predissociated, individual rotational lines can still be identified and used as intermediates in the double resonance experiments. However, the short lifetime of the $\tilde{C}\ ^1B_1$ (1,0,0) rotational levels does require the use of fairly high probe intensities and the careful synchronization of the two lasers. For this report, the data were obtained by using the 0_{00}, 1_{11}, and 2_{02} rotational levels of the $\tilde{C}\ ^1B_1$ (1,0,0) as the intermediates for the double-resonance spectra. The standard notation N_{K_a,K_c}, is used, where N is the total angular momentum minus spin, and K_a and K_c are the projections of N onto the body-frame a and c axes, respectively. In the second stage of the experiments, the probe laser was added and scanned through the wavelength region of interest while monitoring the two-color photoelectron signal. The present study is focused on part of the region between the H_2O^+ $\tilde{X}\ ^2B_1$ (0,0,0) and (1,0,0) ionization thresholds, corresponding to a total energy of 101 800 cm^{-1} to 102 200 cm^{-1}. This energy region should contain $n=6$ Rydberg states with H_2O^+ $\tilde{X}\ ^2B_1$ (1,0,0) ion cores. Finally, the probe laser was tuned to excite a selected autoionizing level in the double resonance spectrum and the photoelectron spectrum was recorded.

The 1-T magnetic field of the electron spectrometer has the potential to distort the ionic rotational distributions, as has been observed in the study of autoionizing states of H_2.[13,14] This effect is not expected to be substantial in the present experiments because the Rydberg states under study have low principal quantum numbers, and because the lifetimes of the autoionizing states are short, thus minimizing the potential effects of such weak interactions. The small effect of the magnetic field in the present studies is supported by the similarity of the $(2+1')$ wavelength scans reported here and the field-free $(1+1')$ wavelength spectra reported by Glab for the same intermediate levels.[11] It should be pointed out, however, that although the same autoionizing levels are observed in both spectra, their relative intensities are somewhat different as a result of the higher probe laser intensities necessary to compete with ionization by the highly focused pump beam in the $(2+1')$ experiments in the magnetic bottle.

III. SPECTROSCOPIC CONSIDERATIONS

The ground state of H_2O has C_{2v} symmetry and the electronic configuration $(1a_1)^2(2a_1)^2(1b_2)^2(3a_1)^2(1b_1)^2$. The outermost orbital is an essentially nonbonding p orbital that lies along the axis perpendicular to the plane of the molecule. The $\tilde{C}\ ^1B_1$ state also has C_{2v} symmetry, with one of the $1b_1$ electrons excited to the $3pa_1$ orbital. The latter is a weakly bonding p orbital that lies along the C_2 axis of the molecule. Excitation of a $1b_1$ electron of the ground state or further excitation of the $3pa_1$ electron of the $\tilde{C}\ ^1B_1$ state results in higher Rydberg states converging to the $\tilde{X}\ ^2B_1$ ground state of H_2O^+. In what follows, a double prime denotes ground state quantities, a single prime denotes $\tilde{C}\ ^1B_1$ quantities, no prime denotes the autoionizing Rydberg state quantities, and a plus denotes ionic quantities.

The geometries of the ground electronic state of the ion and the Rydberg $\tilde{C}\ ^1B_1$ state are very similar. Thus the vibrational wave function overlaps for transitions from the $\tilde{C}\ ^1B_1$ state to high Rydberg states will be large for transitions which occur without a change in vibrational quantum numbers, and much smaller for those involving such a change. This makes it possible to achieve a significant degree of selectivity for the vibrational state of the final Rydberg state by the selection of the vibrational state of the molecule in the intermediate $\tilde{C}\ ^1B_1$ state.[11] This selectivity, taken together with the rotationally resolved stepwise excita-

tion process, results in greatly simplified Rydberg spectra when compared to spectra of excitation directly from the ground state.

The dipole-allowed transitions from the $\tilde{C}\ ^1B_1$ (1,0,0) state to low-lying Rydberg states can be determined relatively simply if the Rydberg states are treated in Hund's case *b*.[24–26] In the coordinate system with *x* along the molecular *c* axis, *y* along the *a* axis, and *z* along the *b* axis, the dipole transition moments T_x T_y, and T_z have b_1, b_2, and a_1 symmetry, respectively. Thus the allowed transitions from the $3pa_1$ orbital of the $C\ ^1B_1$ (1,0,0) state are to be b_1, b_2, and a_1 orbitals and follow type *c* (ΔK_a=odd, ΔK_c=even), type *a* (ΔK_a=even, ΔK_c=odd), and type *b* (ΔK_a=odd, ΔK_c=odd) rotational selection rules, respectively. Note that ΔK_j refers to $K_j - K_j'$ and not $K_j^+ - K_j'$, which is the more relevant quantity in photoionization and in transitions to high Rydberg states and will be referred to as ΔK_j^+.

If the $3pa_1$ orbital of the $\tilde{C}\ ^1B_1$ state was an atomic *p* orbital, only transitions to *ns* and *nd* Rydberg series would be observed. However, the nonspherical nature of the molecular field relaxes this restriction on ℓ, and transitions to *np* and *nf* Rydberg series are also expected. Thus the excitation of a large number of series, corresponding to $nsa_1(\sigma^+)$, $npb_2(\sigma^+)$, $npa_1(\pi^+)$, $npb_1(\pi^-)$, $nda_1(\sigma^+)$, $nda_1(\delta^+)$, $ndb_2(\pi^+)$, $ndb_1(\delta^-)$, $nfb_2(\sigma^+)$, $nfa_1(\pi^+)$, $nfb_1(\pi^-)$, $nfb_2(\delta^+)$, $nfa_1(\phi^+)$, and $nfb_1(\phi^-)$ Rydberg states, is possible. Here λ refers to the projection of ℓ onto the *x* (*a*) axis of the molecule. The large number of allowed levels are expected to make the assignment of the transitions from the $\tilde{C}\ ^1B_1$ state to the low-*n* Rydberg states rather difficult.

As *n* increases, the Rydberg electron uncouples from the molecular frame, resulting in the transition from Hund's case *b* to Hund's case *d*.[8,24] The case *b* states that are described by *N*, K_a, and K_c interact to form Rydberg series converging to distinct N^+, K_a^+, and K_c^+ levels of the ion. Transitions to these higher Rydberg states and to the continua into which they merge must obey selection rules on ΔK_a^+ and ΔK_c^+. These selection rules have been discussed by Lee *et al.* for photoionization from the $\tilde{C}\ ^1B_1$ state[26] and can be expressed

$$\Delta K_a^+ + \ell = \text{odd}, \tag{1}$$

and

$$\Delta K_a^+ + \Delta K_c^+ = \text{even}. \tag{2}$$

Taken together, these selection rules imply that transitions with ΔK_a^+=odd and ΔK_c^+=odd have even ℓ, and those with ΔK_a^+=even and ΔK_c^+=even have odd ℓ. Note, however, that the case *d* states can still be expressed in terms of the case *b* basis, and that type *a*, *b*, and *c* transitions, with their requirements on ΔK_j and not ΔK_j^+, remain allowed. This is consistent with the theoretical direct photoionization calculations of McKoy and co-workers,[18,19,26] who expressed the photoionization matrix elements in terms of body-frame (Hund's case *b*) labels and showed that $k\ell a_1$, $k\ell b_1$, and $k\ell b_2$ partial waves all contribute to the cross section. Continuity arguments imply that partial waves of all three symmetries also contribute to the oscillator strength in the Rydberg series.

Photoelectron spectra obtained for $(2+1')$ excitation via the $\tilde{C}\ ^1B_1$ (0,0,0) state into the direct ionization continuum and the theoretical calculations of these spectra by McKoy and co-workers[18,19,26] provide insight into the relative importance of Rydberg series with different values of *l* in the present $(2+1')$ double-resonance spectra. Glab *et al.* reported extremely good agreement between experiment and theory, indicating that the calculations contain much of the essential physics of the problem.[18,19] Using these calculations, the breakdown of the total cross section into partial cross sections allows the assessment of the relative importance of different partial waves near threshold. These calculations should also provide an indication of which Rydberg series excited from the $\tilde{C}\ ^1B_1$ (1,0,0) state are expected to be strong and which series will be weak. Although the calculations reported by Glab *et al.*[18,19] are for the $\tilde{C}\ ^1B_1$ (0,0,0) state rather than the (1,0,0) state, the electronic factors are not expected to be radically different for the two states. Glab *et al.*[19] reported the theoretical threshold photoionization matrix elements from the $\tilde{C}\ ^1B_1$ (0,0,0) state for all of the allowed partial waves with $\ell \leqslant 3$. Figure 5 of Ref. 19 shows that the $\ell = 3$ matrix elements for one of the kfa_1, kfb_1, and kfb_2 continua are surprisingly large, and that the matrix elements for the *s*, *p*, and *d* continua are all significant. These observations suggest that all of these series will be observable in the excitation spectrum from the $\tilde{C}\ ^1B_1$ level, and that the complete analysis of this spectrum will require that each is taken into account.

Because the initial and final states are the same, the rotational selection rules for photoionization via an autoionizing state are the same as those for direct photoionization.[26,27] Thus the selection rules in Eqs. (1) and (2) provide a connection between the rotationally resolved peaks observed in the photoelectron spectra of autoionizing levels and the partial wave composition of the photoelectron wave function. Given the initial $\tilde{C}\ ^1B_1$ (1,0,0) rotational level, these selection rules imply that, independent of the quantum numbers of the autoionizing level, excitation and decay of autoionizing states with overall with ΔK_a^+=odd and ΔK_c^+=odd produces even ℓ photoelectrons, and that with ΔK_a^+=even and ΔK_c^+=even produces odd ℓ photoelectrons.

IV. RESULTS AND DISCUSSION

A. The $(2+1')$ ionization spectra

Figure 1 shows wavelength scans of the $(2+1')$ ionization spectra via the 0_{00}, 1_{11}, and 2_{02} rotational levels of the $\tilde{C}\ ^1B_1$ (1,0,0) state, in which the integrated two-color photoelectron signal was collected. The selection rule on ΔJ limits the *J* value of the autoionizing resonances to 1; 0, 1, 2; and 1, 2, 3 for the 0_{00}, 1_{11}, and 2_{02} intermediate levels, respectively. The requirements on ΔK_a^+ and ℓ given in Eq. (1) also imply that for a given value of K_a^+, the $J=1$ series accessed from the 0_{00} and 2_{02} rotational levels will have the opposite

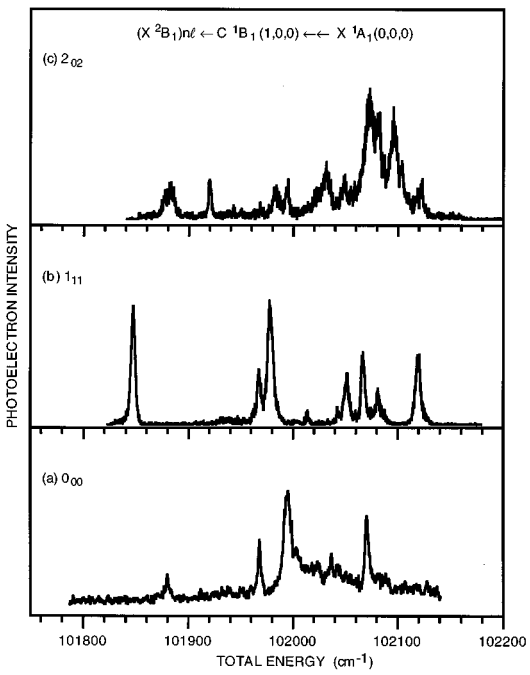

FIG. 1. Wavelength scans of the $(2+1')$ photoelectron signal obtained by pumping selected rotational levels of the $\tilde{C}\ ^1B_1$ (1,0,0) state. (a) The 0_{00} intermediate level; (b) the 1_{11} intermediate level; (c) the 2_{02} intermediate level.

(even/odd) values of ℓ from the $J=1$ series accessed from the 1_{11} level. However, the comparison of the 0_{00} and 2_{02} spectra should allow the assignment of the $J=1$ resonances in the latter.

Apart from these simple considerations, the assignment of the autoionizing resonances in the region between the H_2O^+ $\tilde{X}\ ^2B_1$ (0,0,0) and (1,0,0) thresholds is a nontrivial spectroscopic problem. Although the $(1+1')$ and $(2+1')$ double resonance spectra via selected rotational levels of the $\tilde{C}\ ^1B_1$ state provide important clues for this analysis, in practice the assignment of such spectra remains a significant challenge for theory. To date, the most successful analysis of the resonances in this spectral region has been carried out by using multichannel quantum defect theory (MQDT).[12] In particular, Child and Jungen[8] were reasonably successful in calculating the single-photon ionization spectrum from the $\tilde{X}\ ^1A_1$ (0,0,0) ground state in the region just above the $\tilde{X}\ ^2B_1$ (0,0,0) threshold. In these calculations, Child and Jungen considered only the $nd \leftarrow 1b_1$ transitions, with the assumptions that the $1b_1$ orbital of the ground state is a pure p orbital and that the oscillator strength of the *nd* series dominates that of the *ns* series.[8] The results of these calculations accounted for both the overall appearance and much of the structure in the experimental spectra of Page *et al.* In addition, more refined calculations that included the effects of ℓ mixing (in particular, *s-d* mixing) reproduced many of the features of the higher resolution photoionization data of Vrakking *et al.*[4] Nevertheless, many of the details of the experimental spectra were not reproduced; in addition, the present data require calculations of spectra from the $\tilde{C}\ ^1B_1$ state rather than the $\tilde{X}\ ^1A_1$ state. Although the $3pa_1$ Rydberg electron in the $\tilde{C}\ ^1B_1$ state is also nominally a p electron (calculations by Lee *et al.* give it 77.96% p character),[26] the discussion of the previous section indicates that additional partial waves will be necessary to account for the spectra in Fig. 1.

One of us (MSC) is currently carrying out a detailed MQDT analysis of the spectrum of H_2O excited from the $\tilde{C}\ ^1B_1$ state. This analysis will ultimately include the *s*, *p*, *d*, and *f* Rydberg series, as well as various interactions between the series that result from ℓ uncoupling, Coriolis mixing, etc. In principle, such an analysis can include the calculation of the resonance widths, the ionization efficiency, the branching ratio between ionization and dissociation, and the rotational branching ratios in the photoelectron spectrum.[12] This analysis is not yet complete, and thus the assignment of all of the resonances in Fig. 1 is not possible at this time. However, several of the resonances can be assigned with a good degree of confidence, and the discussion of the photoelectron spectra will focus on these resonances.

The comparison of the spectra of Fig. 1 with $(1+1')$ spectra reported by Glab[11] for the same intermediate states reveals a number of interesting features. In particular, although all of the same resonances are observed, their widths are noticeably greater in the $(2+1')$ spectra. This is a result of the significantly greater probe pulse energy densities necessary to observe a two-color signal when the two-photon pump transition is used: because ionization by the tightly focused pump laser is quite efficient, the higher probe intensities are necessary to compete with one-color ionization. Although the signal-to-noise ratio is not as good, $(2+1')$ spectra recorded with low probe intensities display linewidths and intensities that are in good agreement with the $(1+1')$ spectra. One interesting feature of the higher intensity $(2+1')$ spectra is that the relative intensities of the narrowest peaks in the spectra are significantly smaller than those of the corresponding peaks in the $(1+1')$ or low intensity $(2+1')$ spectra. One explanation for this is that these longer-lived resonances are absorbing an additional photon before they can autoionize. Such an ''above-threshold'' process is expected to result in the production of a new photoelectron peak with higher kinetic energy or to result in the photodissociation of the molecule. The absence of any additional photoelectrons peaks suggests that the photodissociation pathway predominates.

B. Photoelectron spectra of autoionizing levels

The photoelectron spectra in Figs. 2–4 contain information on the possible assignments of the quantum states responsible for different resonances, on the extent of l mixing in the spectrum (which was largely ignored by Vrakking *et al.*[4]), and on the auto-ionization rates in different electronic channels. Our present purpose is to highlight some of the relevant considerations.

Figure 2 shows the photoelectron spectrum for the autoionizing level at a total energy of 101 847 cm^{-1} in the double-resonance spectrum obtained via the $\tilde{C}\ ^1B_1$ (1,0,0) 1_{11} level [see Fig. 1(b)]. The spectrum shows that three H_2O^+ rotational levels are produced, with approximately

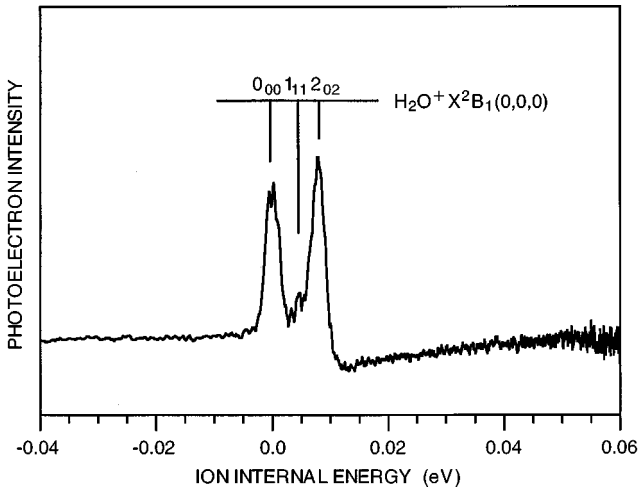

FIG. 2. The photoelectron spectrum for $(2+1')$ excitation via the 1_{11} rotational level of the $\tilde{C}\ ^1B_1$ (1,0,0) state to the $(\tilde{X}\ ^2B_1)6da_1$ (1,0,0) 0_{00} autoionizing resonance at 101 847 cm^{-1} in Fig. 1(b). The ionic rotational levels corresponding to each photoelectron peak are indicated.

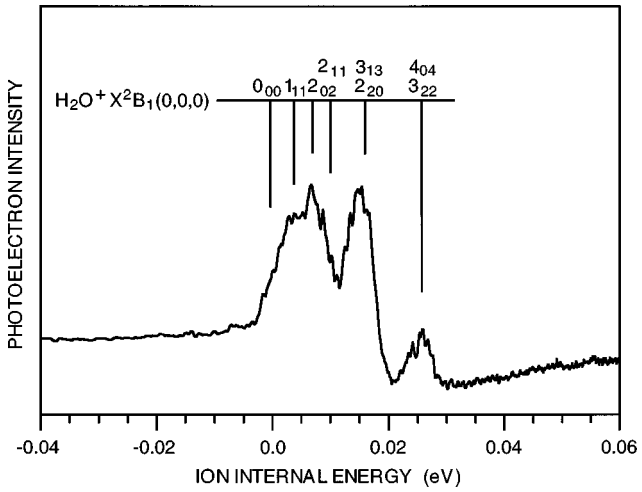

FIG. 4. The photoelectron spectrum for $(2+1')$ excitation via the 1_{11} rotational level of the $\tilde{C}\ ^1B_1$ (1,0,0) state to the $(\tilde{X}\ ^2B_1)6f$ (1,0,0) $J=2$ autoionizing resonance at 101 967 cm^{-1} in Fig. 1(b). The ionic rotational levels corresponding to each photoelectron peak are indicated.

equal populations in the H_2O^+ 0_{00} and 2_{02} levels and a small population in the 1_{11} level. No other H_2O^+ rotational channels are allowed by symmetric and energetic requirements since the resonance energy is only 81 cm^{-1} above the H_2O^+ $\tilde{X}\ ^2B_1$ (0,0,0) 0_{00} ionization limit.

The quantum defects employed by Vrakking *et al.*[4] imply that this resonance should be assigned to the 0_{00}, 2_{02}, or 2_{20} rotational levels of the lower $(\tilde{X}\ ^2B_1)6da_1$ (1,0,0) vibronic state. A preliminary analysis indicates that no *s*, *p*, or *f* Rydberg states are expected within $\sim$100 cm^{-1} of this resonance and the strength of the two major odd ΔK_a^+ and odd ΔK_c^+ photoelectron peaks is consistent, via the selection rules in Eqs. (1)–(2), with an *s* or *d* electronic assignment. The smaller 1_{11} peak then suggests a small admixture of *p* or possibly *f* character.

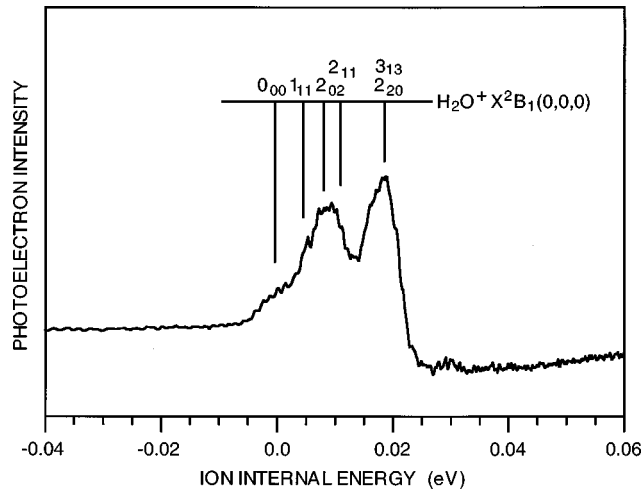

FIG. 3. The photoelectron spectrum for $(2+1')$ excitation via the 0_{00} rotational level of the $\tilde{C}\ ^1B_1$ (1,0,0) state to the $(\tilde{X}\ ^2B_1)6f$ (1,0,0) $J=1$ autoionizing resonance at 101 969 cm^{-1} in Fig. 1(b). The ionic rotational levels corresponding to each photoelectron peak are indicated.

The precise rotational assignment of this $(\tilde{X}\ ^2B_1)6d$ (1,0,0) resonance is more ambiguous. The simplest assignment is to the 0_{00} level, which is consistent with the position and intensity of an observed transition to $(\tilde{X}\ ^2B_1)6da_1$ (1,0,0) 1_{11} via the $\tilde{C}\ ^1B_1$ (1,0,0) 0_{00} level. In this case of vanishing rotational angular momentum, the 0_{00}, 1_{11}, and 2_{02} photoelectron peaks can be immediately associated with *s*, *p*, and *d* photoelectrons, respectively, by the selection rules in Eqs. (1) and (2). In support of this assignment, Vrakking *et al.*[4] did indeed include (10% *s*, 90% *d*) mixing in their analysis, but this alone would not be sufficient to account for the nearly equal intensities of the 0_{00} and 2_{02} photoelectron peaks in Fig. 2. These intensities may indicate that the matrix elements for vibrational autoionization of the ''*s*'' Rydberg states are larger than for the ''*d*'' states, as might be expected for a more penetrating orbital. Alternatively, competing decay processes might reduce the autoionization efficiency of the ''*d*'' component more than the ''*s*'' component.

An alternative assignment of the resonance responsible for the photoelectron spectrum in Fig. 2 is to the 2_{02} rotational level of $(\tilde{X}\ ^2B_1)6da_1$ (1,0,0). The relevant transition from $\tilde{X}\ ^1B_1$ (1,0,0) 1_{11} has the highest calculated rotational line intensity of any transition to $(\tilde{X}\ ^2B_1)6da_1$ (1,0,0) and the case *(d)* composition is roughly equally distributed over the H_2O^+ 0_{00}, 2_{02}, and 2_{20} rotational channels, of which only the first two are open at the energy of this resonance. Redistribution of the 2_{20} population of the open channels would therefore account for the roughly equal intensities of the 0_{00} and 2_{02} peaks, without needing to invoke *s*-*d* mixings. Similar remarks apply to a possible 2_{20} rotational assignment of the resonance, except that the calculated transition intensity is much smaller than for the 2_{02} resonance. Obviously, in the interpretation of the photoelectron spectra, it is important to have a correct identification of the autoionizing state at the outset. Further work on the determination of the state assignments of the resonances is underway, relying

heavily on the high-quality multiple resonance spectra of Ref. 11.

The existence of the weak 1_{11} peak in Fig. 2 implies *p-d* or *d-f* mixing for all three of the possible rotational assignments. Interestingly, Gilbert *et al.*[9] have suggested that *p-d* mixing might account for discrepancies in the experimental and theoretical intensities of the *E* and *E′* bands in the *3d* complex of H_2O. In addition, *p-d* mixing has been used to explain the presence of a number of nominally forbidden transitions in the single-photon ZEKE-PES of the ground state of water.[10] This *p-d* mixing and the nominally forbidden transitions have been explained in terms of mixing induced by the dipole moment of the H_2O^+ ion core, and are fully reproduced in the *ab initio* calculations of Lee *et al.*,[5–7] which treat the molecular field of the core explicitly. In general, however, it is expected that such photoelectron spectra may ultimately provide a more quantifiable handle on such interactions than threshold or ZEKE-PES, in which a large number of effects are known to distort the ''true'' intensities of the different photoelectron peaks,[28–31] that is, the true intensities of the different rotational continua.

Figure 3 shows the photoelectron spectrum for the $J=1$ autoionizing level at a total energy of 101 969 cm^{-1} in the double-resonance spectrum obtained via the $\tilde{C}\ ^1B_1$ (1,0,0) 0_{00} level. MQDT calculations for $n=6-11$ indicate that the observed resonance is a *6f* level; no calculated *s* or *p* resonance was within 50 cm^{-1} of this resonance, and the closest *d* resonance is more than 25 cm^{-1} away. In addition, as is evident in the $(1+1')$ spectrum via the same intermediate level, this resonance is narrower than the other resonances in the 0_{00} spectrum. This behavior is consistent with the assignment as a longer-lived, nonpenetrating *f* state, as opposed to a penetrating *s*, *p*, or *d* state, which would be expected to have a shorter lifetime. The nonpenetrating *nf* Rydberg states of water are expected to be close to Hund's case *(d)*, and the calculations indicate that the observed resonance has an $H_2O^+\ \tilde{X}\ ^2B_1$ (1,0,0) 2_{02} ion core, with case *(d)* quantum numbers $J=1$, $l=3$, $N^+=2$, and $K^+=0$. In the simplest imaginable vibrational autoionization mechanism, this state would autoionize to give $H_2O^+\ \tilde{X}\ ^2B_1$ (0,0,0) 2_{02} with 100% efficiency.

The selection rule in Eq. (1) specifies that for excitation from the 0_{00} level to states with $\ell=$ odd, K_a^+ must be even. Thus, the dominance of the 2_{02} and 2_{20} photoelectron peaks in Fig. 3 is consistent with the assignment of the resonance as an *f* state and with the preservation of ℓ upon autoionization. However, constraints on the total angular momentum ($J=1$) require that the 0_{00} photoelectron peak can only be produced by an $\ell=1$ partial wave. Thus as discussed above, the magnitude of this peak, which appears as a shoulder to the 2_{02} peak, provides a measure of the *p-f* mixing in the autoionizing state. The origin of K_a^+, $K_c^+=$ odd levels in Fig. 3 is not obvious. In particular, the 1_{11} and 2_{11} peaks should appear on opposite sides of the 2_{02} peak, but the latter is not significantly broader than expected, indicating that the K_a^+, $K_c^+=$ odd peaks are relatively weak. Unfortunately, the 3_{13} peak is expected in essentially the same position as the 2_{20} peak, and it will require accurate theoretical calculations to deconvolute any contribution of the former to the spectrum. Restrictions on the total angular momentum indicate that intensity in the 1_{11} peak is correlated with an *s* or *d* photoelectron, intensity in the 2_{11} peak is correlated with a *d* photoelectron, and intensity in the 3_{13} peak is correlated with a *d* or *g* photoelectron.

Figure 4 shows the photoelectron spectrum for the autoionizing level at a total energy of 101 967 cm^{-1} in the double-resonance spectrum obtained via the $\tilde{C}\ ^1B_1$ (1,0,0) 1_{11} level. MQDT calculations indicate that this is also a *6f* resonance but with $J=2$. As in the case of the *6f* resonance excited via the 0_{00} level, this assignment is supported by the observation that this resonance is considerably sharper than most of the other resonances, particularly in the $(1+1')$ spectrum. In Hund's case *(d)*, the dominant contribution to the ion core is from the $H_2O^+\ \tilde{X}\ ^2B_1$ (1,0,0) 1_{11} state, but there is a smaller contribution from the 2_{11} state.

From Eq. (1), autoionization of an *nf* resonance excited from the $\tilde{C}\ ^1B_1$ (1,0,0) 1_{11} level into the ϵf continuum should result in the population of ionic rotational levels with $K_a^+=$ odd ($\Delta K_a^+=$ even). In contrast, the photoelectron spectrum shows significant intensity in both $K_a^+=$ even and odd photoelectron peaks, indicating extensive ℓ mixing. Thus, while the intense 1_{11} photoelectron peak and the contribution of the 3_{13} continuum to the blended 2_{20}, 3_{13} peak are consistent with an ϵf photoelectron, the intense 2_{20} peak and the contribution of the 2_{20} continuum to the blended peak require an ϵs or ϵd photoelectron. Furthermore, the weak, blended 4_{04}, 3_{22} peak and the 0_{00} peak that is a shoulder on the 1_{11} peak can only be explained by even partial waves.

The extensive ℓ mixing required to explain the observed intensity pattern in Fig. 4 is somewhat surprising in light of the relatively minimal ℓ mixing necessary to explain the rotational distributions in Figs. 2 and 3. Even if the assignment of the autoionizing level is incorrect and it is an $\ell=$ even resonance, extensive ℓ mixing must take place. One explanation for this observation is that the autoionizing resonance at 101 978 cm^{-1} contributes to the ionization signal at 101 967 cm^{-1} due to power broadening, and that the former resonance corresponds to an $\ell=$ even level. Alternatively, if the two levels have the same value of *J*, they may interact, and, as a result of their small energy separation, this interaction may be stronger than for the other resonances studied. Such a mechanism requires the two autoionizing resonances have opposite values of ℓ to account for the observed spectrum. It appears unlikely that the ℓ mixing is occurring in the continuum or in the vibrational auto-ionization mechanism because in that case the same mixing would be expected in the photoelectron spectrum of the *6f* resonance in Fig. 3. The observation of extensive ℓ mixing in Fig. 3 points to the need for more detailed theoretical calculations to confirm the identity of the autoionizing resonances and to elucidate the mechanism responsible for the mixing. The experimental photoelectron spectra presented here are expected to provide important guidance in the development of these calculations and in the testing of their accuracy.

V. CONCLUSION

Rotationally resolved photoelectron spectra of rotationally state-selected autoionizing states of water have been re-

ported here for the first time. The spectra, in which even low-J ionic levels are resolved, provide considerable dynamical information on the mechanisms for the transfer of energy and angular momentum between the ion core and the Rydberg electron. The spectra also provide particularly detailed information on the partial-wave composition of the outgoing partial wave. In particular, the photoelectron spectra for $J=0$ autoionizing levels provide a direct partial-wave analysis for the ejected photoelectrons. The observed partial-wave compositions for the spectra reported here can only be explained by invoking varying degrees of *l* mixing brought about by the dipole and higher multiple moments of the H_2O^+ ion core.

While the present experimental results provide substantial insight into the autoionization dynamics, theoretical models and calculations are necessary to extract the full amount of information contained in the spectra. First and foremost, the identification of the autoionizing Rydberg states is necessary before the photoelectron spectra can be put to their best use. An MQDT analysis of the wavelength spectra reported here is currently underway.[32] In addition to the difficulties discussed above, such an analysis may ultimately have to include the possible excitation of Rydberg series converging to the low-lying, linear $\tilde{A}\ ^2A_1$ state,[1,2,4] which can be excited if the core of the $\tilde{C}\ ^1B_1$ state absorbs a photon of suitable energy to promote an electron from the $3a_1$ orbital into the half-filled $1b_1$ orbital. Such Rydberg states are expected to undergo rapid electronic autoionization into the $\tilde{X}\ ^2B_1$ continuum. After the assignment of the wavelength spectra has been completed, MQDT calculations of autoionization rates, rotational branching ratios, and ionization efficiencies will allow a much fuller comparison between experiment and theory, and will ultimately lead to a much better understanding of the decay dynamics of the Rydberg states of polyatomic molecules.

ACKNOWLEDGMENTS

W.L.G. was partially supported by the Robert A. Welch Foundation. S.T.P. was supported by the U.S. Department of Energy, Office of Energy Research, Office of Basic Energy Sciences, Division of Chemical Sciences, under Contract No. W-31-109-Eng-38.

[1] R. H. Page, R. J. Larkin, Y. R. Shen, and Y. T. Lee, J. Chem. Phys. **88**, 2249 (1988).
[2] P. M. Dehmer and D. M. P. Holland, J. Chem. Phys. **94**, 3302 (1991).
[3] R. G. Tonkyn, R. Wiedmann, E. R. Grant, and M. G. White, J. Chem. Phys. **95**, 7033 (1991).
[4] M. J. J. Vrakking, Y. T. Lee, R. D. Gilbert, and M. S. Child, J. Chem. Phys. **98**, 1902 (1993).
[5] M. T. Lee, K. Wang, V. McKoy, R. G. Tonkyn, R. T. Wiedmann, E. R. Grant, and M. G. White, J. Chem. Phys. **96**, 7848 (1992).
[6] M. T. Lee, K. Wang, and V. McKoy, J. Chem. Phys. **97**, 3108 (1992).
[7] K. Wang, M. T. Lee, V. McKoy, R. T. Wiedmann, and M. G. White, Chem. Phys. Lett. **219**, 397 (1994).
[8] M. S. Child and Ch. Jungen, J. Chem. Phys. **93**, 7756 (1990).
[9] R. D. Gilbert, M. S. Child, and J. W. C. Johns, Mol. Phys. **74**, 473 (1991).
[10] R. D. Gilbert and M. S. Child, Chem. Phys. Lett. **287**, 153 (1991).
[11] W. L. Glab, J. Chem. Phys. **107**, 5979 (1997).
[12] C. H. Greene and Ch. Jungen, Adv. At. Mol. Phys. **21**, 51 (1985).
[13] J. L. Dehmer, P. M. Dehmer, S. T. Pratt, F. S. Tomkins, and M. A. O'Halloran, J. Chem. Phys. **90**, 6243 (1989).
[14] S. T. Pratt, E. F. McCormack, J. L. Dehmer, and P. M. Dehmer, J. Chem. Phys. **92**, 1831 (1990).
[15] H. Park, D. J. Leahy, and R. N. Zare, Phys. Rev. Lett. **76**, 1591 (1996).
[16] H. Park and R. N. Zare, J. Chem. Phys. **106**, 2239 (1997).
[17] W. L. Glab, P. M. Dehmer, and J. L. Dehmer, J. Chem. Phys. **104**, 4937 (1996).
[18] W. L. Glab, P. T. Glynn, P. M. Dehmer, J. L. Dehmer, K. Wang, and B. V. McKoy, J. Chem. Phys. **106**, 5779 (1997).
[19] W. L. Glab, P. T. Glynn, P. M. Dehmer, J. L. Dehmer, K. Wang, and V. McKoy, in preparation.
[20] P. Kruit and F. H. Read, J. Phys. E **16**, 313 (1983).
[21] J. E. Reutt, L. S. Wang, Y. T. Lee, and D. A. Shirley, J. Chem. Phys. **85**, 6928 (1986).
[22] H. Lew, Can. J. Phys. **54**, 2028 (1976).
[23] M. N. R. Ashfold, J. M. Bayley, and R. N. Dixon, Chem. Phys. **84**, 35 (1984).
[24] G. Herzberg, *Molecular Spectra and Molecular Structure, Vol. III* (Van Nostrand Reinhold, New York, 1966).
[25] J. T. Hougen, J. Chem. Phys. **37**, 1433 (1962).
[26] M. T. Lee, K. Wang, V. McKoy, and L. E. Machado, J. Chem. Phys. **97**, 3905 (1992).
[27] R. Signorell and F. Merkt, Mol. Phys. **92**, 793 (1997).
[28] K. Müller-Dethlefs and E. W. Schlag, Annu. Rev. Phys. Chem. **42**, 109 (1991).
[29] W. A. Chupka, J. Chem. Phys. **98**, 4520 (1993).
[30] F. Merkt and T. P. Softley, Int. Rev. Phys. Chem. **12**, 205 (1993).
[31] G. P. Bryant, Y. Jiang, M. Martin, and E. R. Grant, J. Phys. Chem. **96**, 6875 (1992).
[32] M. S. Child (in preparation).